Shock-induced termination of cardiac arrhythmias

Group members: Baltazar Chavez-Diaz, Chen Jiang, Sarah Schwenck, Weide Wang, and Jinglei Zhang

Abstract:

Cardiac arrhythmias occur when blood flow to the heart is disrupted by irregular electrical activity. To treat these arrhythmias, the irregular activity must be removed and regular activity recovered. This is usually done using defibrillation, where a controlled amount of energy is delivered to the heart. There are three basic protocols of defibrillation: monophasic, which consists of one phase; symmetrical biphasic, which consists of two equal phases; and asymmetrical biphasic, which has two unequal phases. In order to determine the efficiency of each of these three protocols, we modelled the membrane potential by combining three partial differential equations. These equations were broken down into ordinary differential equations and solved through matlab. A matrix of voltage at each individual time step during the shock was used to determine success of failure of the defibrillation. As before, the monophasic protocol was found to be most efficient as lower energies, while asymmetrical biphasic was the most efficient as mid to high levels at energy. At high levels of energy (E>7V/cm), all three protocols had greater than 90% successful defibrillations.

Introduction:

Cardiac arrhythmias, also known as irregular heartbeat, occur when the electrical activity of the heart is irregular, disrupting the flow of blood to the heart[1]. Arrhythmias can result in either the heart beating too quickly as in ventricular tachycardia, or too slowly, as in bradycardia[2]. While many arrhythmias are not life-threatening, they are still a leading cause of morbidity and mortality. In fact, over 300,000 individuals die suddenly yearly in the United States, and in most cases it is thought that arrhythmias are the cause[2]. Furthermore, the Center for Disease Control estimated that 2.66 million people would have atrial fibrillation in 2010, indicating that they are a world-wide problem[2].

Now, the pumping of the heart is controlled through electrical impulses. Specialized cells within the right atrium known as the sinoatrial node fire spontaneously about 70 times per minute[2]. These firings lead to the coordinated contraction of the atria and then, after a slight delay, the ventricles. As a result, in order to treat cardiac arrhythmias, the irregular electrical activity must be removed and the regular activity recovered.

Defibrillation is commonly used to terminate cardiac arrhythmias such as ventricular tachycardia[3]. Defibrillation consists of delivering a controlled amount of electrical energy to the heart using a device called a defibrillator. This suppresses the chaotic cardiac action potentials caused by the arrhythmia and allows the normal rhythm to be reestablished[3]. There are three main protocols commonly used in commercial defibrillators, which are based on monophasic and both symmetric and asymmetric biphasic shocks. The monophasic protocol consists of only one

phase while the biphasic consists two phases, where the polarity of the electrodes is switched during the second phase. Biphasic shocks can be either symmetrical or asymmetrical, and the asymmetrical shocks can have either a shorter first or second phase. Biphasic shocks are thought to be more efficient than monophasic shocks based upon empirical evidence found by Ideker's group in the late 1980s[3]. However, it is not yet fully understood why biphasic shocks are more efficient. As a result, in our project, we will quantitatively compare the efficiency of the three different protocols.

Our model uses the simplest geometry that can maintain a propagating action potential- a one-dimensional ring of cardiac tissue (see Figure 1)[3]. Under normal circumstances, an action potential is initialized and travels around the ring. In our case, the shock will be modeled as the application of currents through electrodes on either side of the ring. These electrodes can either inject or subtract electrical charges during the shocks. A defibrillatory shock will be defined as successful if all wave propagation is removed within one second of the end of the shock[3]. If any wave activity is still present, the shock will be characterized as unsuccessful.

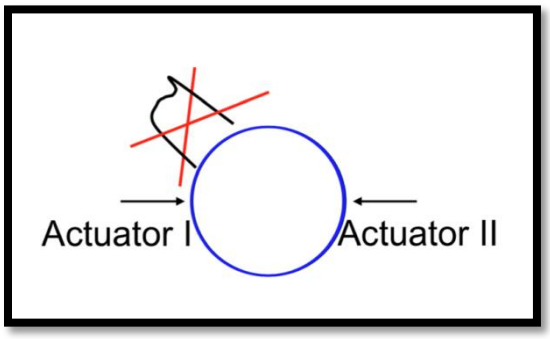

Figure 1. Schematic of the ring of cardiac tissue. The two areas represent the locations of the two electrodes.

Because wave propagation determines success or failure, action potential waves, which show how membrane potential changes when the defibrillatory shock is applied, are important. Now, membrane potential refers to the difference in electric potential between the inside and the outside of cells. In humans, there is a much higher proportion of sodium (Na^+) outside the cell than in and much more potassium (K^+) inside the cell than out[5]. As a result, sodium moves into the cell and potassium out via ion channels according to their concentration gradients. In addition, membrane potentials are usually held stable at around -70 to -80 millivolts[5]. However, when this potential rises past a certain threshold, an action potential can occur. Action potentials occur in several types of cells, including neurons, muscle cells and endocrine cells. During action potentials, the membrane potential of the cells changes as the cell is first depolarized by the opening of voltage-gated Na^+ channels and then repolarized by the opening of voltage-gated K^+ channels (see Figure 2)[5]. Following an action potential, there is a refractory period where the potential falls below the resting potential. This prevents the action potential from travelling the opposite direction and continues the flow of information through the cells.

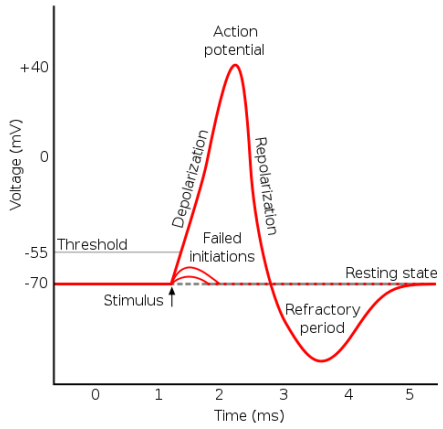

Figure 2. A typical action potential showing first the depolarization and then repolarization stages.

Methods:

By expanding upon the Beeler-Reuter equations, which describe the electrical activity of cardiac myocytes, the membrane potential can by calculated by solving:

(1) $\frac{\partial V_m}{\partial t} = -\frac{I_{BR}+I_{ep}+I_{fu}}{C_m} + \nabla \cdot \left(D_g \cdot \nabla V_m\right) + \nabla \cdot (D_g \cdot \nabla \varphi_e)$

where V_m is the membrane potential[3,4]. This equation was solved in matlab by using the matlab package ODE23 to solve for the ordinary differential equations I_{ep}, I_{fu}, and φ_e.

In equation (1), C_m represents the capacitance of the myocyte membrane, or its ability to store charge, I_{BR} is the membrane current, I_{ep} is the current associated with electroporation, and I_{fu} accounts for the possible stimulation of the tissue through an anode break. Looking first at I_{BR}, we can split this term into four parts:

(2) $I_{BR} = I_K + I_x + I_{Na} + I_s$

In this case, I_K and I_X both represent potassium currents outward, I_{Na} represents the sodium current in, and I_S represents the calcium current inward. I_X and I_{Na} represent the currents generated during an action potential by the opening of voltage-gated sodium and potassium channels and I_K represents the current caused by the presence of leaky potassium channels in the cells which are consistently letting small amounts of potassium out of the cell.

Each of these four currents was modelled as in Courtemanche[6] and was computed using matlab package ODE23 as follows:

(3) $I_k = 40.35\frac{e^{0.04*(V(i,j)+85)}-1}{e^{0.08*(V(i,j)+53)}+e^{0.04*(V(i,j)+53)}} + 0.2*0.35\frac{(V(i,j)+23)}{1-e^{-0.04(V(i,j)+23)}}$

(4) $I_X = 0.8x\frac{e^{0.04(V(i,j)+77)}-1}{e^{0.04(V(i,j)+35)}}$

(5) $I_{Na} = (g_{Na}m^3hj + g_{NaC})(V(i,j) - E_{Na})$

(6) $I_S = g_S df(V(i,j) - E_S)$

where $g_{Na} = 4\ \frac{mS}{cm^2}$, $g_{NaC} = 0.003\ \frac{mS}{cm^2}$, $g_S = 0.09\frac{mS}{cm^2}$, $E_{Na} = -50\ mV$, and $E_S = -82.3 - 13.0287\ \ln(c)$. The calcium concentration *c* also satisfies

(7) $\frac{dc}{dt} = -10^{-7} I_S + 0.07(10^{-7} - c)$

Now while equation (3) is time independent, equations (4-6) all contain a time independent variable. These are gating variables (*m, h, j, x, d,* and *f*), which model the opening and closing of ion channels in the cells. All of these variables were solved by equations of the form:

(8) $\frac{dx}{dt} = \frac{x_\infty - x}{\tau_x}$

(9) $x_\infty = \frac{\alpha_x}{\alpha_x + \beta_x}$

(10) $\tau_x = \frac{1}{\alpha_x + \beta_x}$

where α and **β** are constants for each of the six variable listed above. These constants depend on voltage and are given by

$$\alpha_x = \frac{0.0005e^{0.083(V(i,j)+50)}}{1 + e^{0.057(V(i,j)+50)}} \qquad \beta_x = \frac{0.0013e^{-0.06(V(i,j)+20)}}{1 + e^{0.04(V(i,j)+20)}}$$

$$\alpha_m = \frac{V(i,j) + 47}{1 - e^{-0.1(V(i,j)+47)}} \qquad \beta_m = 40e^{-0.056(V(i,j)+72)}$$

$$\alpha_h = 0.126e^{-0.25(V(i,j)+77)} \qquad \beta_h = \frac{1.7}{1 + e^{-0.082(V(i,j)+22.5)}}$$

$$\alpha_j = \frac{0.055e^{-0.25(V(i,j)+78)}}{1 + e^{-0.2(V(i,j)+78)}} \qquad \beta_j = \frac{0.3}{1 + e^{-0.1(V(i,j)+32)}}$$

$$\alpha_d = \frac{1}{\sigma}\frac{0.095e^{-0.01(V(i,j)-5)}}{1 + e^{-0.072(V(i,j)-5)}} \qquad \beta_d = \frac{1}{\sigma}\frac{0.07e^{-0.017(V(i,j)+44)}}{1 + e^{0.05(V(i,j)+44)}}$$

$$\alpha_f = \frac{1}{\sigma}\frac{0.012e^{-0.008(V(i,j)+28)}}{1 + e^{0.15(V(i,j)+28)}} \qquad \beta_f = \frac{1}{\sigma}\frac{0.0065e^{-0.02(V(i,j)+30)}}{1 + e^{-0.2(V(i,j)+30)}}$$

where V(i,j) is the voltage inputted in to the system and **σ** = 0.5. By computing the constants α and **β**, we are able to solve for each of the variables *m, h, j, x, d,* and *f* using equations (8), (9), and (10). Thus, we can calculate equations (3-6) and solve for I_{BR}.

Next, I_{ep} accounts for the electroporation phenomenon. This phenomenon occurs when a shock is applied and results in the creation of pores in the membrane of the cell. These pores allow for ion flow which prevents the membrane potential from reaching an unrealistic level. I_{ep} was modelled by solving the equation

(11) $$I_{ep} = g_p(V_m)NV_m$$

where g_p is the conductance of a single pore and N is the total number of pores per unit of membrane area. Also, I_{ep} is only included if the membrane potential is greater than 180mV or less than -150mV, as these are values that would not usually be found in the cells. As a result, at those membrane potentials, pores would be created to rebalance the membrane potential.

Finally I_{fu} accounts for the possible anode break stimulation and was modelled by solving

(12) $$I_{fu} = F * \left(V(i,j) - E_f\right) * 0.1$$

where E_f is the reversal potential and F is a gating variable determined by the following equations:

$$\frac{dF}{dt} = \frac{F_\infty - F}{F}$$

$$F_\infty = \frac{\alpha_F}{\alpha_F + \beta_F}$$

$$\tau_F = \frac{1}{\alpha_F + \beta_F}$$

Here, α_F and $\boldsymbol{\beta}_F$ are constants given by

$$\alpha_F = 0.01824e^{\frac{-V(i,j)+170}{12.36}} \quad \text{and} \quad \beta_f = \frac{-0.074655}{1 + e^{\frac{V(i,j)-29.056}{27.7}}} + 0.075955$$

Moving on to the next two partial differential equations in equation (1), φ_e represents the extra-cellular potential and D_g denotes intra-cellular diffusion of the electrical potential. The second term, $\nabla \cdot \left(D_g \cdot \nabla V_m\right)$, describes the diffusion of the potential from the inside of the cell out. By taking the divergence of this term, we can understand how the diffusion is changing with time. Similarly, the third term, $\nabla \cdot (D_g \cdot \nabla \varphi_e)$, describes the diffusion from the outside of the cell into the cell over time. In order to solve equation for the third term, we solved for φ_e in matlab by solving the Poisson equation

(13) $$\nabla \cdot \left[\left(D_e + D_{g)} \cdot \nabla \varphi_e\right] = -\nabla \cdot \left(D_g \cdot \nabla \mathrm{V_m}\right) - \frac{I_{ext}}{\beta C_m}$$

Here, I_{ext} is the extracellular current and D_e and D_g are extra-cellular and intra-cellular diffusion respectively. We set $D_e = D_g = 1.5 * 10^{-3}$ cm^2ms^{-1}.

Thus, by recursively solving for equation (1), we obtained time steps of voltage that produce a matrix of voltage at each individual time step. This matrix allows us to determine the success or failure of the defibrillation. By running multiple simulations, an average of successful defibrillations was determined and color plots of successful defibrillations for each protocol were created.

Now, within our model, we will be considering seven main parameters that can influence the success or failure of defibrillation. The first is the shock waveform, or the three basic protocols of defibrillation described above. The second, shock duration, refers to how long the shock is applied. As in the simulations done by Bragard *et al.*, this was kept constant. Next,

shock energy refers to how strong the shock is. The strength of the shock was varied from E= 1 V/cm to E= 10V/cm. Next, shock timing refers to the location of the action potential wave front and back at the time of the shock. The size of the action potential is also important in determining defibrillation outcome as it is constantly varying as the dynamics are quasi-periodic. The heterogeneity of the cardiac tissue also plays a role as heterogeneities create more polarization sites within the tissue which makes excitation easier. Finally, the system size, or the size of the ring, plays a role. The system size in our model will be set to 6.7 cm, as was done by Bragard *et al.* In addition, our spatial discretization is 0.025cm. Also, during the first ten milliseconds of the shock, the time step with be set to 0.001 milliseconds. At every time following, it will be set to 0.01 milliseconds.

Results:

The monophasic protocol was found to be most efficient at the lowest energy (E =1) (see Figure 3a-c). For each plot, successful defibrillation is shown through a color gradient, where red indicates 100% success and blue indicates 0% success. Because a larger area of the figure is red for the monophasic protocol, this indicates that a greater proportion of the defibrillations are successful (Figure 3a). However, for each of the three protocols at low energy, a large proportion of the figure is blue, indicating that all three protocols are not successful very often.

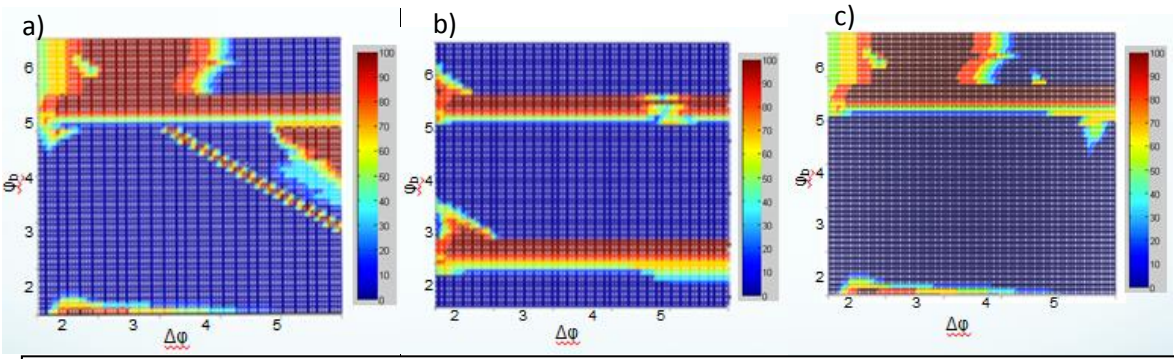

Figure 3. Color plot of successful defibrillations for (a) monophasic, (b), symmetrical biphasic, and (c) asymmetrical biphasic for E-=1v/cm.

At higher energy, when E= 3V/cm, all three protocols were about equal efficiency, but the asymmetrical biphasic protocol was found to be the most efficient (see Figure 4c, Table 1). All protocols were more efficient than when E=1V/cm (Figure 4a-c). This is shown by the greater proportion of the plots being redder than they were for the lower energy, indicating that overall, a greater amount of the defibrillations are successful at this higher energy.

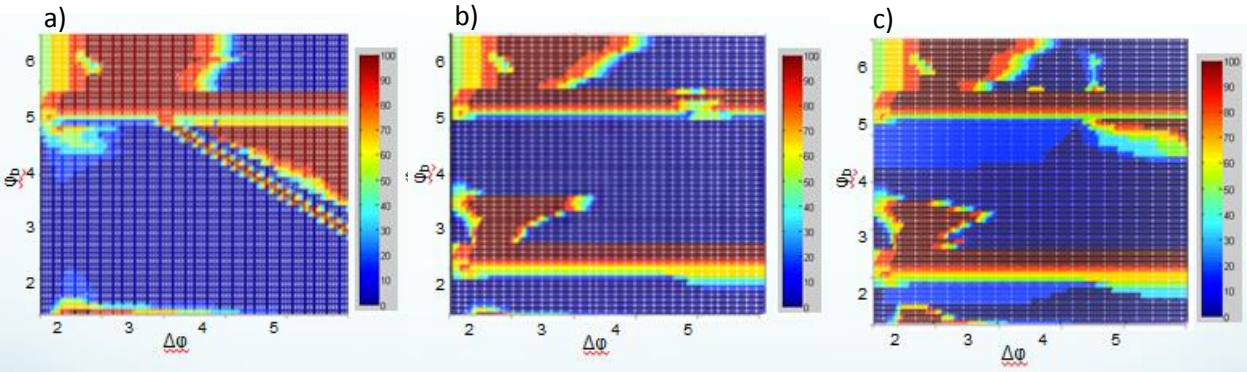

Figure 4. Color plot of successful defibrillations for (a) monophasic, (b), symmetrical biphasic, and (c) asymmetrical biphasic for E-=3v/cm.

When the energy was increased even higher, the relative difference between the three protocols increased, with the asymmetric biphasic protocol being the most efficient, and monophasic being the least efficient (see Table 1). Also, with each sequential increase in energy, the percent of successful defibrillations increased. Consequently, at energy levels above 7 V/cm, all three protocols had successful defibrillations more than 90% of the time (see Table 1).

Table 1. Percent of successful defibrillations for energy levels of 1, 3, 7, and 9 V/cm.

E (V/cm)	Monophasic	Symmetric Biphasic	Asymmetric Biphasic
1	28	17	16
3	44	43	45
7	93	99	98
9	99	100	100

Conclusions:

As in Bragard *et al*., it was determined that monophasic shocks were the most efficient at lower energies, while otherwise, the asymmetrical biphasic was the most efficient. While this indicates asymmetric biphasic shocks are more efficient than monophasic shocks, this model is not directly applicable to real life as different values of energy are inputted, since monophasic and biphasic defibrillators are classified based on the amount of joules they dispense, rather than volts (monophasic dispenses 150J, biphasic 200J). However, when considering the relative increase in efficiency between the monophasic and biphasic shocks, both the model and previous experiments show about a 25% increase. Thus, this model is a promising first step to more advanced models of defibrillations.

Additionally, we were not able to fully compare our model to that of Bragard *et al*., as we were not able to classify our successful defibrillations into the four mechanisms as defined by Bragard *et al.* Consequently, we were only able to compare each of the three protocols to determine which was more effective overall, but we were not able to determine what types of mechanisms dominant at each energy level. Furthermore, the one-dimensionality of our model

limits its accuracy when compared to experimental results, as human tissues are not one-dimensional. However, this model is simple and cost-effective, allowing numerous simulations to be run. However, because of that, we are also not able to account for shocks that may cause fibrillation instead of defibrillation, as is sometimes seen in medical experiments.

References:

1. Center for Disease Control. (2010). Atrial Fibrillation Fact Sheet.
2. Keating, M. T. and Sanguinetti, M. C. (2001). Molecular and cellular mechanisms of cardiac arrhythmias. Cell. 104, 569-580.
3. Bragard, J. *et al.* (2013). Shock-induced termination of reentrant cardiac arrhythmias: Comparing monophasic and biphasic shock protocols. Chaos: An Interdisciplinary Journal of Nonlinear Science 23).
4. Beeler, G.W. and Reutter, H. (1977). Reconstruction of the action potential of ventricular myocardial fibers. Journal of Physiology 268, 177-210.
5. Barnett, M.W. and Larkman, P.M. (2007). The action potential. Practical Neurology 7, 192-197.
6. Courtemanche, M. (1996). Complex spiral wave dynamics in a spatial distributed ionic model of cardiac electrical activity. Chaos: An Interdisciplinary Journal of Nonlinear Science 6, 579-600.